



Collective modes and Raman scattering in one dimensional electron systems

D.-W. Wang^{a,*}, A.J. Millis^b, S. Das Sarma^c

^a*Department of Physics, Harvard University, Cambridge, MA 02138, USA*

^b*Department of Physics, Columbia University, New York, NY 10027, USA*

^c*Condensed Matter Theory Center, Department of Physics, University of Maryland, College Park, MD 20742, USA*

Received 30 March 2004; accepted by the guest editors

Available online 15 June 2004

Abstract

In this paper, we review recent development in the theory of resonant inelastic light (Raman) scattering in one-dimensional electron systems. The particular systems we have in mind are electron doped GaAs based semiconductor quantum wire nanostructures, although the theory can be easily modified to apply to other one-dimensional systems. We compare the traditional conduction-band-based non-resonant theories with the full resonant theories including the effects of interband transitions. We find that resonance is essential in explaining the experimental data in which the single particle excitations have finite spectral weights comparable to the collective charge density excitations. Using several different theoretical models (Fermi liquid model, Luttinger liquid model, and Hubbard model) and reasonable approximations, we further demonstrate that the ubiquitously observed strong single particle excitations in the experimental Raman spectra cannot be explained by the spinless multi-spinon excitations in the Luttinger liquid description. The observability of distinct Luttinger liquid features in the Raman scattering spectroscopy is critically discussed.

© 2004 Published by Elsevier Ltd.

PACS: 71.45. – d; 73.20.Mf; 73.20.Dx; 78.30.Fs; 78.30. – j

Keywords: A. Semiconductor; E. Inelastic light scattering

1. Introduction

One-dimensional (1D) electron systems, where electron dynamics is constrained to be along a single direction (chosen as the x axis in the rest of this paper where necessary) due to the quantum mechanical confinement of the carrier system imposed by suitable externally applied electrostatic potentials along y and z directions (leaving the x direction to be the only direction of free-electron-like motion characterized by a 1D wavevector k), have been achieved in the electron-doped GaAs quantum wire structures by combining the state of the arts semiconductor materials growth with extremely clever nanolithographic

fabrication technique [1]. In these 1D semiconductor quantum wire structures the non-interacting 3D electron wavefunction can be described, to a very good level of accuracy, using the effective mass approximation [2–4] as $\Psi(\mathbf{r} = (x, y, z)) = \tilde{\Psi}_j(y, z)e^{ikx}/\sqrt{L_x}$, where L_x is the plane wave normalization length along the wire direction, x , and $\tilde{\Psi}_j(y, z)$ is the bound wavefunction for electron motion in the quantized transverse (y – z) direction with j denoting a particular bound state [2] for the y – z motion. The transverse bound states (usually called ‘subbands’ in the semiconductor literature [2,5]) characterized by the discrete index j ($= 0, 1, 2, \dots$ with 0 being the ground state lying lowest in energy near the conduction band minimum of GaAs) are typically separated by a few meV in energy with their separation (as well as the carrier density in the system) being somewhat tunable through various gate voltages applied from outside. For low temperature (≤ 1 K), $k_B T \ll (E_1 - E_0)$

* Corresponding author. Tel.: +1-617-495-0843; fax: +1-617-496-2545.

E-mail address: dwwang@cmt.harvard.edu (D.W. Wang).

where E_j is the j th subband energy for transverse motion and therefore $(E_1 - E_0)$, the lowest intersubband energy separation, is the low-lying excited state energy, the quantum wire system is by definition, a strictly one-dimensional quantum mechanical electron system at low carrier densities [i.e. for $E_F < (E_1 - E_0)$] so that only the lowest quantum level, the ground subband, is occupied by electrons. Even in a situation where $E_F > (E_j - E_0)$ for a few values of j , the semiconductor quantum wire system is a ‘multisubband’ 1D electron system [5] as long as the intersubband scattering between different subbands is relatively weak (which is usually the case).

Such 1D semiconductor quantum wires, particularly in their strict 1D one-subband [i.e. $E_F < E_1 - E_0$] limit, are examples of interacting 1D electron systems, the so-called Tomonaga–Luttinger liquids (‘Luttinger liquids’), which are of great intrinsic and fundamental interest in condensed matter physics [6–9]. In particular, Luttinger liquids (LL) are fundamentally different from Fermi liquids (i.e. interacting 2D and 3D electron systems such as normal metals and two-dimensional electron systems confined in semiconductor heterostructures) in the sense that the one-to-one correspondence between the interacting (‘Fermi liquids’) and the non-interacting (‘Fermi gas’) systems, which is the basis of the very successful Landau Fermi liquid (FL) theory in two- and three-dimensional electron systems, categorically breaks down for 1D Luttinger liquids. As a result, one-dimensional electron systems do not have a Fermi surface defined by a finite jump of momentum distribution, n_k , at Fermi wavevector at zero temperature even in the presence of weak interactions (more precisely, if one defines the Fermi surface to be a singularity of n_k , at $|k| = k_F$, then 1D interacting electron systems can still have a Fermi surface due to the infinite slope of n_k at $|k| = k_F$), i.e. interaction effects are non-perturbative in one-dimensional electron systems.

Luttinger liquids (i.e. interacting 1D electron systems) are characterized by the absence of long wavelength low energy single particle (i.e. electron–hole) excitations which dominate the low energy spectra of 2D and 3D systems and by the existence of spin–charge separation, i.e. separate branches of low energy excitations in Luttinger liquids can carry spin but no charge (‘spinons’) or can carry charge but no spin (‘holons’) in contrast to higher dimensional systems where the single-particle excitations necessarily carry both spin and charge. The zero-temperature momentum distribution function in Luttinger liquids does not have the usual discontinuity at $k = k_F$ indicating the existence of a Fermi surface, but instead has a power-law behavior $n(k - k_F) \sim 1/2 - \text{sgn}(k - k_F)|k - k_F|^\alpha$, where the exponent (the so-called Luttinger exponent) is non-universal.

In this paper we review our recent theoretical work on the inelastic resonant light (‘Raman’) scattering studies of 1D semiconductor quantum wires, using both the Fermi liquid and the Luttinger liquid approaches. Resonant Raman scattering (RRS) has been a very successful tool for

studying the elementary electronic excitation spectra in doped semiconductors. In particular, the mode dispersion (i.e. the frequency as a function of wavevector) and the spectral weight (i.e. the oscillator strength) of low energy (from a fraction of an meV to tens of meV) electronic excitations can be directly obtained via resonant Raman scattering (in the 10^5 – 10^6 cm^{-1} wavevector range). Since the interesting and important elementary electronic excitations in GaAs quantum wire (1D) and quantum well (2D) structures lie precisely in this frequency–wavevector range, resonant Raman scattering spectroscopy has been an effective tool for studying electronic excitation spectra in GaAs based low dimensional electron systems over the last twenty-five years [5,10–12,15]. In addition, various selection rules involving the relative polarization of the incident and scattered photons in the Raman spectra (the so-called polarized or the depolarized spectra) allow one to study charge density or spin density excitations in the system, making the resonant Raman scattering spectroscopy a rather powerful tool for studying intra- and inter-subband electronic excitations in 1D and 2D electronic systems including the strongly correlated fractional quantum Hall regime [13].

The Raman scattering spectra, within the simple linear response theory, is directly proportional to the dynamical structure factor of the interacting electron system which, at long wavelength, has significant spectral weight only at collective excitations, if no inter-subband resonant scattering involved [5,16–18]. Depending on the polarization configuration of the experimental set up, the Raman scattering spectra should directly measure either the collective charge density excitation (in the polarized or the non-spin–flip configuration) or the collective spin density excitation (in the depolarized or the spin–flip configuration) [10,11,14,15]. Within the simple linear response theory [5,16–18], the Raman scattering spectra in the two configurations is simply proportional to the imaginary part of the screened (for the charge density excitation (CDE) in the polarized configuration) or unscreened (for the spin density excitation (SDE) in the depolarized channel) polarizability function. At very small wavevectors that can be probed in the Raman scattering experiments, only the collective modes should have appreciable spectral weight in the Raman scattering spectra. This fact, i.e. that only collective modes (either CDE in the polarized spectra or SDE in the depolarized spectra) can manifest themselves in the inelastic light scattering spectra of semiconductor structures applies to systems of any dimensionality, 3D, 2D or 1D electron systems [5,17–19]. Of course, in principle, the incoherent single particle excitations (electron–hole pairs) can be also observed in the Raman scattering experiment of two- and three-dimensional system with small (but finite) momentum transfer, due to the existence of quasi-particle excitations. In one-dimensional electron system, on the other hand, only collective charge and spin modes are expected to be

observed since the single particle excitations are absent in the LL theory as we mentioned above.

A real intriguing aspect of the resonant inelastic light scattering spectroscopy in semiconductor structures has, however, been the persistent and ubiquitous presence of a ‘single-particle excitation’ (SPE) peak in the Raman scattering spectra in sharp contradiction with the simple theoretical description provided above. This single particle excitation peak, which is usually fairly weak (but orders of magnitude stronger than that given by the simple electronic response function argument given above), is almost always present in the resonant Raman scattering spectra in addition to the expected peaks associated with the collective excitations [11,12,14,15,20,21]. A very interesting aspect of this phenomenon is the fact that collective mode spectral features in the resonant Raman scattering spectra seem to be rather well-described by the simple response theory, which at the same time predicts orders of magnitude weaker values for the single particle spectral weight (in 2D and 3D) than that observed experimentally. In 1D semiconductor quantum wire structures, where the Luttinger liquid behavior manifestly precludes the existence of low-lying single particle excitations, the observed existence of SPE features in the Raman scattering spectra [11,14,21] raises very serious conceptual questions regarding our basic understanding of the elementary excitation spectra in 1D electron systems.

In this review we discuss how this conceptual problem has recently been resolved theoretically by showing that a full understanding of the existence of single particle excitation like spectral features in the resonant Raman scattering spectra necessarily requires going beyond the simple non-resonant single band (i.e. conduction band) linear response theory and considering the full ‘two-step’ resonant aspect of the experiment (Fig. 1(a)) where the valence band plays a crucial role [22]. For completeness we will first review the theories of non-resonant Raman

scattering using 1D FL model, LL model, and lattice Hubbard model, respectively. We then discuss the theories of resonant Raman scattering including the two-step scattering process. Finally, we discuss how these results are related to the existing experimental data and their implication to the Luttinger liquid properties in 1D electron-doped semiconductor quantum wire systems.

In Fig. 1(a) we depict the schematic diagram [23] for the two steps involved in the resonant Raman scattering process: an electron in the valence band is excited by the incident photon into the conduction band above Fermi surface, leaving a valence band hole behind (step 1), and then an electron from inside the conduction band Fermi surface recombines with the hole in the valence band (step 2), emitting an outgoing photon with an energy and momentum (Stokes) shift. (In principle, these two steps could occur in different orders). The net result is an elementary electronic excitation created in the conduction band through the intermediate valence band states. The non-resonant approximation to RRS ignores the intermediate valence band states as shown by the step 3 in Fig. 1(a). Note that the resonant process depends on the incident photon energy, while the non-resonant approximation depends only on the energy difference between the incident and the scattered photons. This difference turns out to be crucial in the RRS theory as shown below. Total electron spin is conserved in the final scattering processes since we are considering only the polarized geometry (i.e. photon polarization is not changed). We restrict ourselves to the non-spin-flip polarized RRS, where the CDE dominates the non-resonant linear response spectra.

2. Non-resonant Raman scattering theory

In the presence of an external photon field the interaction between the electron gas and the radiation field is described by the following Hamiltonian:

$$H = H_e + \sum_i^N \left[-\frac{e}{m_i c} \mathbf{p}_i \cdot \mathbf{A}_i + \frac{e^2}{2m_i c^2} \mathbf{A}_i^2 \right] \quad (1)$$

where $\mathbf{A}_i = \mathbf{A}(\mathbf{x}_i, t)$ is the vector potential of photon, \mathbf{x}_i and \mathbf{p}_i are the position and momentum operators of i th electrons, and c is the speed of light. m_i is the effective electron mass in the semiconductor bands (m_i can be different if considering interband scattering). H_e is the Hamiltonian of electrons interacting with Coulomb potential without the radiation field. Fig. 1(b) and (c) correspond to the scattering processes induced by the linear ($\mathbf{p} \cdot \mathbf{A}$) term and the quadratic (\mathbf{A}^2) term respectively in the second quantization representation. One can simply neglect the $\mathbf{p} \cdot \mathbf{A}$ term in Eq. (1) if only the non-resonant Raman scattering spectroscopy is considered, where the incident photon frequency is far away from the band gap energy [24,25]. The resulting Raman scattering intensity therefore is equivalent to the imaginary part of the

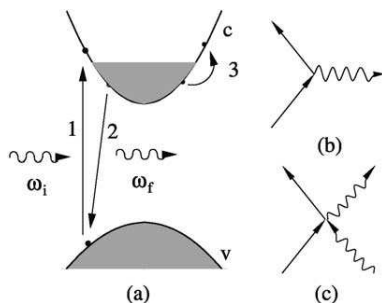


Fig. 1. (a) Schematic representation of the two-step RRS in the direct gap two band [c(v): conduction (valence) band] model. ω_i and ω_f are the initial and final frequencies of the external photons. (b) and (c) are the Feynman diagrams of the electron–photon scattering process described by $\mathbf{p} \cdot \mathbf{A}$ and $\mathbf{A} \cdot \mathbf{A}$ terms respectively in the interacting Hamiltonian (see text). Solid and wavy lines represent the electron and photon Green’s functions respectively.

time-ordered density correlation function in the linear response theory [16,26]:

$$\text{Im} \left[i \int_{-\infty}^{\infty} dt e^{i\omega t} \langle T[n^\dagger(k, t)n(k, 0)] \rangle_0 \right] \quad (2)$$

where $\langle \dots \rangle_0$ is the ground state expectation value, and $n(k, t)$ is the electron density operator. In the rest of this section, we will compare the results of Eq. (2) calculated by different theoretical models.

2.1. Fermi liquid model

In the Fermi liquid model [16], the elementary excitations of an interacting electronic system are quasi-particles, which have the same quantum numbers as free electrons but with an effective mass and renormalized single particle parameter. It is well-known that the Fermi liquid model is a very good approximation in two and three dimensional systems, but fails in one dimensional systems due to strong fluctuations. However, it has also been noticed that [19,27] the collective plasmon modes calculated by the standard random phase approximation (RPA) within the FL model is exactly the same as the one obtained by Luttinger liquid model (see below). Its energy dispersion is $\omega_p(k) = v_F |k| \sqrt{1 + 2V_c(k)/\pi v_F}$, where v_F is Fermi velocity and $V_c(k) \propto \ln(1/kd)$ is the 1D Coulomb interaction with d being the characteristic confinement length in the transverse dimension. Therefore it is instructive to compare the RRS spectrum calculated in the FL model within RPA to the results obtained by other exactly solvable models in 1D electron system (see below).

In Fig. 2, we show the typical non-resonant Raman scattering spectra calculated in the FL model within RPA (solid lines). It shows a strong CDE spectral weight at the plasmon mode energy, and a much weaker (three orders in magnitude) weight in the single particle excitation (SPE)

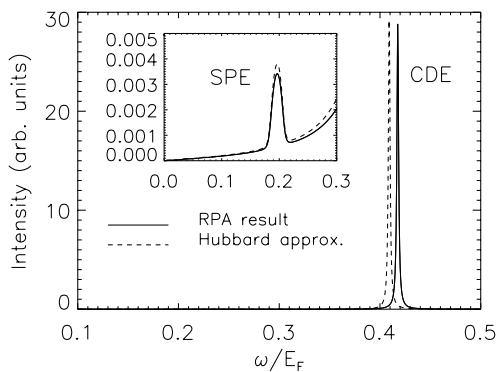


Fig. 2. Dynamical structure factor of a 1D electronic systems obtained by the standard (non-resonant) RPA calculation at $k = 0.1k_F$. The electron densities used in the calculation is $6.5 \times 10^5 \text{ cm}^{-1}$. Finite impurity scattering ($\gamma = 10^{-3} E_F$) has been applied to broaden the peaks.

energy, $\omega = kv_F$. The almost vanishing weak presence of the SPE peak results from the quasi-particle excitations in the FL model. The dashed lines in the same figure are results calculated by including vertex corrections (within Hubbard approximation [19,28]) in the theory to go beyond the RPA approximation. We find that the simple non-resonant vertex correction still gives qualitatively the same result with a SPE spectral weight orders of magnitude weaker than the CDE. Including the effects of non-parabolicity of the electron band energy and/or the effects of the breakdown of electron momentum by scattering with impurity potential can enhance the SPE weight slightly (less than one order of magnitude) but still does not change the picture qualitatively [19]. Thus, possible adjustments and improvements of the theory staying within the conduction band non-resonant Raman scattering picture are not capable of explaining the experimental observation of a strong presence of the SPE spectral feature in the RRS spectra [14].

2.2. Luttinger liquid model

The Luttinger liquid model [6–9] is thought to provide a generic low energy description for 1D electron systems, which are characterized by the LL fixed point in the renormalization group sense. The standard and exactly solvable LL model is the 1D electron gas with a linear dispersion ($E_k = rv_F(k - rk_F)$) around Fermi points ($\pm k_F$) at each branch ($r = \pm 1$) and with short-ranged forward interaction [6,7]. It is well-known [7] that the exactly diagonalized LL Hamiltonian consists of two independent elementary excitations: charge bosons (holons) and spin bosons (spinons), the so-called spin–charge separation. The former is essentially equivalent to the spinless charge density excitations of the FL model with the same plasmon velocity, while the latter occurs in the depolarized (spin–flip) scattering channel at the Fermi velocity, and is akin to the spin density excitation mode of the FL. Therefore, in the non-resonant polarized Raman scattering spectroscopy we consider in this paper, the LL model has only the charge boson (plasmon) excitations, and does not have any single particle weight due to the breakdown of Landau Fermi liquid in 1D system. However, including the non-linearity of the band energy may lead to situation where the charge mode and the spin mode sectors interact with each other and cause possible multi-boson excitation above the Fermi surface. It has been proposed [29] that a spin singlet excitation (SSE) of two bound spinons (of total spin zero) may be responsible for the observed single particle excitation in the Raman scattering experiments. It is therefore important to study how such multi-boson excitations affect the polarized spectrum in an exactly solvable model with a non-linear band energy. We therefore consider the 1D Hubbard model in Section 2.3 in this context, considering in details its excitation spectra. Although the lattice Hubbard model does not really apply to continuum semiconductor quantum wire systems, generic LL

properties (e.g. the excitation spectra and spectral weights) should be independent of the model.

2.3. Hubbard model

The exactly solvable 1D single band Hubbard model (HM) contains a hopping matrix element between neighboring sites, t , and a spin-dependent on-site interaction, U . The full Hamiltonian is

$$H = -t \sum_{i,\sigma} (c_{i+1,\sigma}^\dagger c_{i,\sigma} + \text{H.c.}) + U \sum_i n_{i\uparrow} n_{i\downarrow} \quad (3)$$

where $c_{i,\sigma}$ and $n_{i,\sigma}$ are respectively the fermion creation operator and the density operator for site i and spin σ . Among the many accurate and useful methods to study the 1D HM, we use the Bethe–ansatz method [30–32] to obtain the ground state and the low-lying excitation spectra. Since the Bethe–ansatz wavefunctions are not particularly useful in calculating the correlation functions, we use the Lanczos–Gagliano (LG) diagonalization method [19,33] to directly calculate the spectral weights of these elementary excitations. Our results obtained by this technique are consistent with the quantum Monte Carlo calculations [34] where appropriate. We note that analytic low energy behaviors of some correlation functions of 1D Hubbard model have been calculated in Ref. [43].

In Fig. 3(a), we show the energy–momentum dispersion obtained from the poles of the imaginary part of the charge density correlation function together with the results calculated by Bethe–ansatz equations. The center of each open diamond represents the position of the pole, and its area is proportional to the spectral weight of that excitation. We find that the charge density excitations (often these excitations are called holons or particle-hole excitations in the Bethe–ansatz literature [8,31]) cover almost exactly the same region including the energy minimum at $4k_F$ except for the lower-lying peaks around $2k_F$, where the singlet spinon just matches those peaks. In Fig. 3(b), we show the imaginary part of the charge density correlation function of the same system at $k = 2\pi/9$. It shows that singlet spinons have a relatively small but non-negligible weight (different from the results of FL and LL models), compared with the weight of the dominant charge density excitations (holons). Their relative spectral weight ratio is less than 0.1. We have also studied the dispersions and spectral weights of different filling factors and/or different interaction strengths (for more details, see Ref. [19]), but do not see any possibility to obtain a reasonable fit of the ‘two peak’ RRS structure observed in Ref. [14]. Therefore, we conclude that although the non-parabolicity of the electron conduction band and the spin-dependent interaction contained in the Hubbard model enhance the spectral weight of the singlet spinon excitations (which can be interpreted as the SPE feature in the RRS experiments), the present results obtained without resonance effects cannot explain the experimental data in the RRS

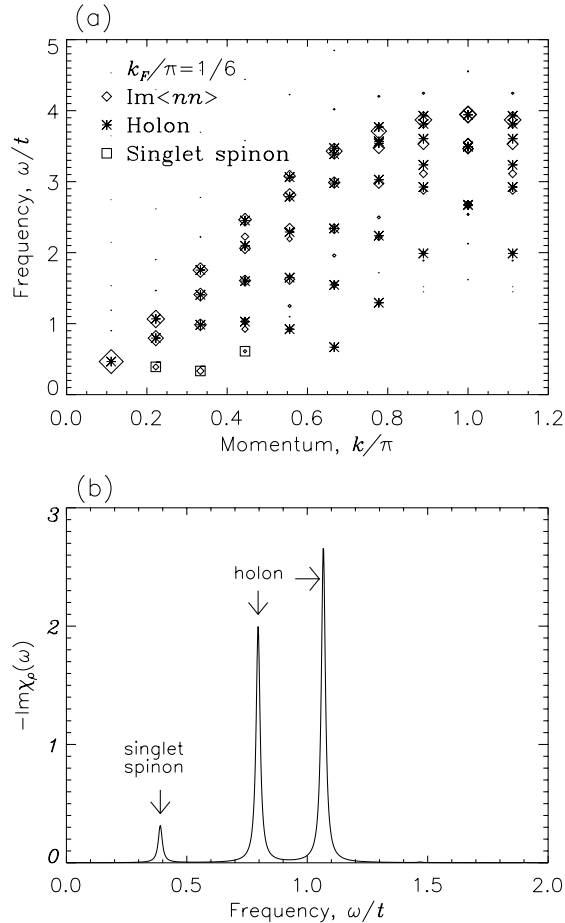


Fig. 3. (a) Energy-momentum dispersion and (b) the spectrum of charge density correlation function of 1D HM for 6 electrons in 18 sites with $U/t = 3$. $k = 2\pi/9$ for the spectrum (b). Holon excitations here are equivalent to the charge density excitations in the Raman scattering experiments. The area of each diamond (square) in (a) is proportional to the spectral weight of each charge (spin) excitation peak.

experiments. The obtained SPE-like RRS feature cannot be explained by staying within a single band LL model.

3. Resonant Raman scattering theory

We now consider the full resonance situation (step 1 and 2 in Fig. 1) of a Raman scattering process by including the valence band explicitly [20,22,23,35]. When the incident photon energy is near the $E_0 + \Delta_0$ direct gap, the second order perturbative contribution of the $\mathbf{p}\cdot\mathbf{A}$ term in Eq. (1) becomes important and comparable to the first order contribution of the \mathbf{A}^2 term, leading to an electron interband transition between the conduction band and the valence

band. The finite time duration between the first step and the second step of the scattering process gives a non-trivial contribution to the scattering matrix element. The transition rate in the second order perturbation theory can be obtained to be [36] (we assume the electron–photon coupling vertex to be a constant for simplicity)

$$W = \lim_{T \rightarrow \infty} \frac{1}{T} \sum_{\mathbf{p}_1, \mathbf{p}_2, \sigma_1, \sigma_2} \int_{-T/2}^{T/2} dt_1 \int_{-T/2}^{t_1} dt_2 \int_{-T/2}^{t_2} dt_1' \times \int_{-T/2}^{t_1'} dt_2' e^{i\bar{\omega}(t_2' - t_1' + t_1 - t_2)} e^{i\bar{\omega}(t_2 + t_1' - t_1 - t_2)/2} e^{iE_{\mathbf{p}_1}^v(t_1' - t_2')} e^{iE_{\mathbf{p}_3}^v(t_1 - t_2)} \times \langle c_{\mathbf{p}_1 + \mathbf{q}/2, \sigma_1}(t_2') c_{\mathbf{p}_1 - \mathbf{q}/2, \sigma_1}^\dagger(t_1') c_{\mathbf{p}_2 - \mathbf{q}/2, \sigma_2}(t_1) c_{\mathbf{p}_2 + \mathbf{q}/2, \sigma_2}^\dagger(t_2) \rangle_0 \quad (4)$$

where we have chosen the backward scattering channel $\mathbf{k}_i = -\mathbf{k}_f = \mathbf{q}/2$ and $\omega_{i,f} = \bar{\omega} \pm \omega/2$, without any loss of generality. $E_{\mathbf{p}}^v$ is the band energy of electrons in the valence band. This result can be evaluated within the Fermi liquid model and the Luttinger liquid model independently and we present these results respectively in the following sections. In Eq. (4) and the following formula in the FL model, we keep the vector form of the momentum indices because they apply equally well to two- and three-dimensional systems.

3.1. Fermi liquid model

As mentioned above, in the FL model, the single particle energy is assumed to be well-defined, so that one can easily integrate out the time difference between the absorption and the emission of the external photon and obtain [36]

$$W(q, \omega; \Omega) = \int_{-\infty}^{\infty} dt e^{i\omega t} \langle N^\dagger(\mathbf{q}, t) N(\mathbf{q}, 0) \rangle_0 \quad (5)$$

where the resonant ‘density’ operator, $N(\mathbf{q}, t)$, is defined to be $N(\mathbf{q}, t) = \sum_{\mathbf{p}, \sigma} A(\mathbf{p}, \mathbf{q}) c_{\mathbf{p} + \mathbf{q}/2, \sigma}^\dagger(t) c_{\mathbf{p} - \mathbf{q}/2, \sigma}(t)$ with the matrix element $A(\mathbf{p}, \mathbf{q})$

$$A(\mathbf{p}, \mathbf{q}) = \frac{1}{-\Omega + (1 + \xi)(E_{\mathbf{p}}^c - E_F) + E_{\mathbf{q}}^c/4 + i\lambda} \quad (6)$$

Here $\Omega \equiv \bar{\omega} - E_g - (1 + \xi)E_F$ is the mean photon energy relative to the resonance energy, and $\xi \equiv m_c/m_v$ is the ratio of the carrier effective mass in conduction and valence bands; $E_F = E_{k_F}^c = k_F^2/2m_c$ is the Fermi energy of the conduction band electrons. λ is a phenomenological broadening parameter we introduce to include roughly all possible broadening effects during the resonance scattering process. (A microscopic evaluation of λ seems to be essentially impossible at the present time [37].)

Comparing Eq. (2) with Eq. (5), we find that the resonance effect on the conduction band electrons is in the matrix element $A(\mathbf{p}, \mathbf{q})$, which arises from the time difference between the two steps of Raman scattering. In the following discussion we define ‘off resonance’ as $|\bar{\Omega}| > E_F$ and ‘near resonance’ as $|\bar{\omega}| \ll E_F$. Off resonance the spectral weight decreases as $|\bar{\Omega}|^{-2}$, while near resonance the

singular properties of $A(\mathbf{p}, \mathbf{q})$ strongly enhance the spectral weight non-trivially. The calculation of the RRS spectrum is therefore reduced to the evaluation of the correlation function of Eq. (5), which can be easily calculated within the RPA approximation [36].

In Fig. 4, we show a typical result of the resonance Raman scattering spectra in the polarized channel. We find that the resonance effects strongly enhance the SPE spectral weight near resonance ($|\bar{\Omega}| \leq 0.1E_F$), making the SPE weight even larger than the CDE spectral weight. Off resonance ($|\bar{\Omega}| > 0.1E_F$), the SPE weights become much smaller than the CDE weight very similar to the non-resonance situation. We note that the Raman energy shift is not affected by resonance effects and hence the one-band non-resonant linear response theory still well-describes the spectral peak energy dispersions. This agrees well with the existing RRS experimental data [14,15,21].

3.2. Luttinger liquid model

The general formula of Raman scattering spectra, Eq. (4), can also be evaluated within the LL model. Using the space-time translational symmetry, Eq. (4) can be simplified by

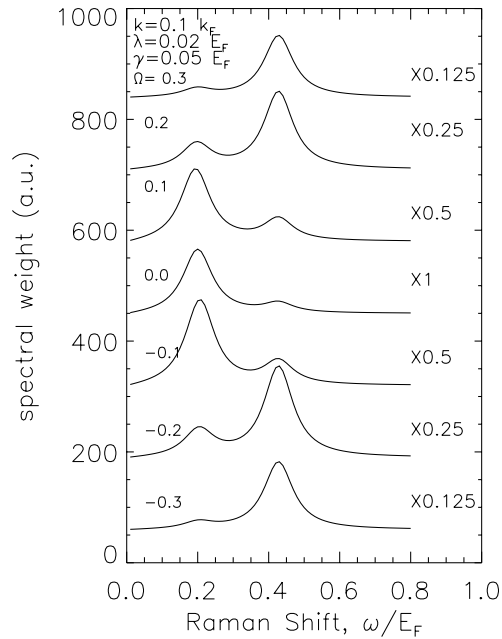


Fig. 4. Raman scattering spectrum near resonance calculated in the FL model. Finite impurity scattering (γ) has been included to broaden the resonance peak properly. Other system parameters are the same as used in Fig. 2. Note that the scales of each plot are indicated in the right hand sides.

representing the fermion operators in the coordinate space:

$$W(q, \omega; \Omega) = \int dRdT e^{i(\omega T - qR)} \langle \hat{O}^\dagger(R, T) \hat{O}(0, 0) \rangle_0 \quad (7)$$

where

$$\hat{O}(R, T) = \sum_{r,s} \int dx \int_0^\infty dt \phi(x, t) \psi_{r,s}(R + x/2, T + t/2) \times \psi_{r,s}^\dagger(R - x/2, T - t/2) \quad (8)$$

$\psi_{r,s}$ is the electron operator for the left ($r = -1$) and the right ($r = +1$) fermion branch of spin index s . The retardation function, $\phi(x, t)$ is

$$\phi(x, t) = \frac{e^{i\omega t}}{L} \sum_p e^{i(E_p^v t - px)} = e^{i(\Omega + v_F^v k_F)t} \delta(x + rv_F^v t) \quad (9)$$

where we have used the linearized valence band energy around the Fermi wavevector, and v_F^v is the associated valence band velocity. Eqs. (8)–(9) are the fundamental results of the RRS theory in the LL model. They show that the RRS process creates an electron–hole pair separated in space by x and in time by t , with the amplitude for a given space–time separation controlled by the function $\phi(x, t)$. Far from resonance, $\phi(x, t)$ is short ranged in both x and t , so that \hat{O} becomes similar to the ordinary density operator and W becomes the charge density correlation function [35,36] (e.g. Eq. (2)). As the mean photon energy is tuned closer to the resonance condition, $\phi(x, t)$ becomes longer ranged, and then \hat{O} becomes non-local in both space and time. Similar to the FL model, this non-locality will be seen to give rise to the interesting resonance effects, by allowing the light to couple to something other than the dynamical structure factor, making the situation qualitatively different from the non-resonant one-band situation.

Although in principle Eq. (7) can be reduced further by using the bosonization method and then calculated numerically, it is more instructive to consider their leading order contributions from the one-boson and two-boson excitations [35]. The former is directly related to the usual plasmon mode excitation (i.e. CDE) in the FL-RPA theory, and the latter is associated with the singlet two-spinon excitations at $\omega = qv_F$. The analytical results for these two leading order contributions can be also obtained [35,38], and one finds that the spectral weight of the charge boson mode (i.e. CDE) decreases as $|\Omega|^{2\alpha-2}$ at off resonance [35,39] where $\alpha \in [0, 1]$ is the Luttinger liquid exponent which is positive for repulsive interaction. In Fig. 5, we show the calculated polarized LL RRS spectra including one and two boson contributions for different resonance conditions. One observes that near resonance the ‘SPE’ peak (now it is composed by two spinon excitations) is noticeable, but still has rather weak spectral weight compared with the CDE (charge boson) peak. This is because any resonance enhanced single particle excitation during the RRS process will be immediately separated into spin and charge channels

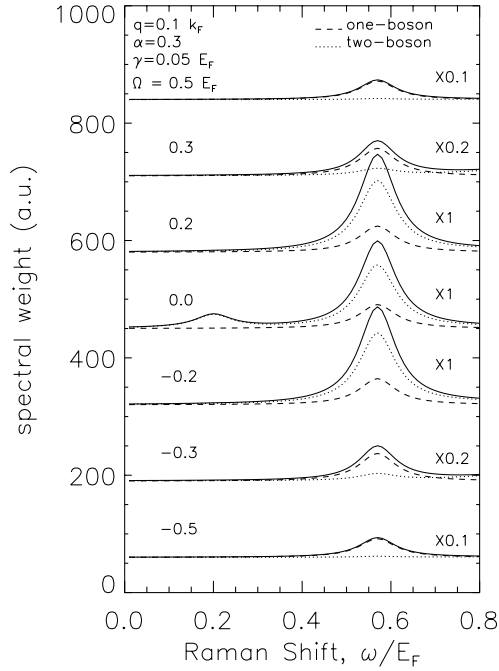


Fig. 5. Calculated polarized RRS spectra for various resonance condition, Ω , in LL model. One- and two-boson contributions have been plotted separately in order to show their relative contributions. The Fermi velocity is the same as used in Fig. 4, while the short-ranged interaction strength is chosen to $\alpha = 0.3$.

in the LL model due to the spin–charge separation. The angular momentum conservation imposed selection rules for non-spin–flip scattering processes automatically suppress the single spin-boson contribution, so that only the singlet spinon excitations (composed by at least two spinons) can contribute to the spectral weight. Therefore, the strongly suppressed ‘SPE’ mode in the polarized spectrum near resonance may possibly be a characteristic LL signature in the semiconductor quantum wire systems.

We also have studied the transition rate, Eq. (7), by summing all higher order results beyond the leading one and two boson contributions. We find that [38] the spectral weight of the total charge boson excitation (i.e. CDE) is still much larger than the total singlet spinon excitation (SSE) in the parameter regime of the existing experiments. The ratio (CDE/SSE) becomes close to unity only near the non-interacting limit, but increases when the electron–electron interaction becomes stronger. We have also considered the situation of the long-ranged Coulomb interaction rather than the short-ranged interaction extensively used in the standard LL model. We find that the SSE spectral weight is further suppressed by the long-ranged Coulomb interaction, showing that the weak singlet spinon excitations in the polarized RRS spectroscopy are generic features of the LL model. Therefore we conclude that the experimental RRS results obtained so far in the literature [11,14,21] are not decisive

signatures of Luttinger liquids in the semiconductor quantum wires since the SSE spectral weight seems to remain somewhat weak in the LL theory compared with the RRS observations (and the SSE is really the only available candidate for the SPE seen in the RRS spectra within the LL model).

4. Discussion

As we have mentioned briefly in the context of Eq. (9), the most significant feature of an RRS process is the retardation effect between the two steps of scattering (see Fig. 1), which is completely absent in the non-resonant theory [19]. Such retardation effects can be studied within the FL model in all dimensions [36] or within the LL model in the one-dimensional system [35]. The polarized RRS spectra calculated in both models (FL and LL) are very similar far from resonance: the main contribution is from the collective CDE plasmon mode (or charge boson) excitation at plasmon energy, $\omega = \omega_p(q)$, but a relatively small (but finite) single particle excitation (or the singlet spinon excitation in LL model) can also appear at energy, $\omega = |q|v_F$. However, close to the resonance, the results calculated by these two models are quite different: The SPE weight in the FL model can become comparable to the collective CDE mode weight, whereas the weight of SSE in the LL model is always smaller than the charge boson weight [37,38].

Therefore, a crucial question is the extent to which Raman scattering experiments reveal LL features characteristic of the one dimensional physics. The differences between a Luttinger liquid and a Fermi liquid are most evident in the single electron problem, which is measurable in principle by photoemission [40] or tunneling [41] experiments but is unfortunately not directly measurable by non-resonant Raman scattering, which involves the creation of particle-hole pairs in the conduction band. However, the situation can be different when considering the resonance feature explicitly, because only single electron (not charge or spin bosons) excitations between the conduction band and valence band are possible. Therefore, from the perspective of single particle properties, we suggest that the RRS process near the resonance condition can in principle be also a tool to experimentally distinguish the Luttinger liquid behavior from the Fermi liquid behavior. We note that far away from resonance, the photon frequency dependence of the spectral weight of the CDE mode is different in these two models: it scales as $|\Omega|^{-2}$ in the FL theory, but decreases slower as $|\Omega|^{2\alpha-2}$ in the LL theory [39].

The LL calculations predict a much smaller relative spectral weight in the SPE mode compared with the CDE mode than that observed in the existing experiments. This disagrees with the conclusion in Ref. [22], where the resonance matrix elements are not self-consistently treated

in the Luttinger liquid theory [35]. It is possible that the experiments are not yet probing the low energy limit where the Luttinger liquid model is fully applicable. This can be attributed to, for example, the finite size effects of the wire, finite band curvature for excitations about the Fermi surface, and/or finite temperature cut-off, etc. All of which may suppress the LL features in the experiment making it indistinguishable from the FL theory results.

5. Summary

In this paper, we review the various theories for the resonant Raman scattering experiment, a powerful tool to study the elementary electronic excitations in low-dimensional semiconductor structures. In addition to the known collective plasmon (charge boson) excitations, the Luttinger liquid can in principle have an additional singlet spinon excitation which could mimic the single particle excitation behavior in the Fermi liquid model. The polarized RRS spectra calculated in the FL model and the LL model, however, are different in the relative weights of these excitations with the FL model in general showing much better agreement with experiment. This may be because the strong interband scattering invariably present in the resonant process mixes the conduction band and the valence band states together, leading to an ‘imperfect’ one-dimensional system for electron excitations near the conduction band Fermi surface (i.e. electrons can be excited from below the conduction band Fermi surface to above the Fermi surface via the mediation of the valence band). However, in our present theory, we do not, include excitonic effects (interaction between conduction band electrons and valence band holes) in calculation, which might be crucial during the Raman scattering process near resonance conditions. Therefore, further theoretical and experimental studies are required for the unambiguous demonstration of the Luttinger liquid behavior in the RRS spectra of the semiconductor quantum wire structures. This somewhat unclear RRS situation, where the Fermi liquid model seems to produce apparent better quantitative agreement with the experimental observations in GaAs quantum wires, is in sharp contrast with the tunneling spectroscopic transport studies of GaAs quantum wires [41] which are well-explained by the Luttinger liquid theory [42].

This review is a brief summary of our recent works in the Raman scattering theory of one-dimensional electronic systems (Refs. [19,23,35,36,38]). Readers can find more details and references therein.

References

- [1] See, for example (a) Y.C. Chang, L.L. Chang, L. Esaki, Appl. Phys. Lett. 47 (1985) 1324. (b) A.R. Gofii, K.W. West, A.

- Pinczuk, H.U. Baranger, H.L. Stormer, Appl. Phys. Lett. 61 (1992) 1956.
- [2] W.Y. Lai, S. Das Sarma, Phys. Rev. B 33 (1986) 8874.
- [3] (a) Q.P. Li, S. Das Sarma, Phys. Rev. B 43 (1991) 11768. (b) Q.P. Li, S. Das Sarma, R. Joynt, Phys. Rev. B 45 (1992) 13713.
- [4] (a) S. Das Sarma, D.-W. Wang, Phys. Rev. Lett. 84 (2000) 2010. (b) D.-W. Wang, S. Das Sarma, Phys. Rev. B 64 (2001) 195313.
- [5] S. Das Sarma, Elementary excitations in low-dimensional semiconductor structures, in: D.J. Lockwood, J.F. Young (Eds.), Light Scattering in Semiconductor Structures and Superlattices, Plenum, New York, 1991, p. 499.
- [6] (a) S. Tomonaga, Prog. Theor. Phys. 5 (1950) 544. (b) J.M. Luttinger, J. Math. Phys. NY. 4 (1963) 1154. (c) F.D.M. Haldane, J. Phys. C 14 (1981) 2585.
- [7] J. Voit, Rep. Prog. Phys. 58 (1995) 977.
- [8] H.J. Schulz, in: V.J. Emery (Ed.), Correlated Electron Systems, World Scientific, Singapore, 1993.
- [9] G.D. Manhan, Many Particle Physics, Plenum, New York, 1990.
- [10] A. Pinczuk, B.S. Dennis, L.N. Pfeiffer, K.W. West, Phil. Mag. B 70 (1994) 429 and references therein.
- [11] A. Schmeller, A.R. Goi, A. Pinczuk, J.S. Weiner, J.M. Calleja, B.S. Dennis, L.N. Pfeiffer, K.W. West, Phys. Rev. B 49 (1994) 14778.
- [12] (a) J.E. Zucker, A. Pinczuk, D.S. Chemla, A.C. Gossard, Phys. Rev. B 35 (1987) 2892. (b) G. Danan, A. Pinczuk, J.P. Valladares, L.N. Pfeiffer, K.W. West, C.W. Tu, Phys. Rev. B 39 (1989) 5512–5515.
- [13] (a) I. Dujovne, A. Pinczuk, M. Kang, B.S. Dennis, L.N. Pfeiffer, K.W. West, Phys. Rev. Lett. 90 (2003) 036803. (b) A. Pinczuk, J.P. Valladares, D. Heiman, A.C. Gossard, J.H. English, C.W. Tu, L. Pfeiffer, K. West, Phys. Rev. Lett. 61 (1988) 2701. (c) A. Pinczuk, B.S. Dennis, L.N. Pfeiffer, K. West, Phys. Rev. Lett. 70 (1993) 3983.
- [14] A.R. Goñi, A. Pinczuk, J.S. Weiner, J.M. Calleja, B.S. Dennis, L.N. Pfeiffer, K.W. West, Phys. Rev. Lett. 67 (1991) 3298.
- [15] C. Schüller, G. Biese, K. Keller, C. Steinbach, D. Heitmann, Phys. Rev. B 54 (1996) R17304.
- [16] D. Pines, P. Nozieres, The Theory of Quantum Liquids, Benjamin, New York, 1966.
- [17] (a) J.K. Jain, P.B. Allen, Phys. Rev. Lett. 54 (1985) 947. (b) J.K. Jain, P.B. Allen, Phys. Rev. Lett. 54 (1985) 2437. (c) S. Das Sarma, E.H. Hwang, Phys. Rev. Lett. 81 (1998) 4216.
- [18] (a) J.K. Jain, S. Das Sarma, Phys. Rev. B 36 (1987) 5949. (b) J.K. Jain, S. Das Sarma, Surf. Sci. 196 (1988) 466. (c) J.K. Jain, P.B. Allen, Phys. Rev. Lett. 54 (1985) 947. (d) S. Das Sarma, P. Tamborenia, Phys. Rev. Lett. 73 (1994) 1971.
- [19] D.W. Wang, S. Das Sarma, Phys. Rev. B 65 (2002) 035103.
- [20] B. Jusserand, M.N. Vijayaraghavan, F. Laruelle, A. Cavanna, B. Etienne, Phys. Rev. Lett. 85 (2000) 5400.
- [21] J. Rubio, J.M. Calleja, A. Pinczuk, B.S. Dennis, L.N. Pfeiffer, K.W. West, Solid State Commun. 125 (2003) 149–153.
- [22] M. Sasseti, B. Kramer, Phys. Rev. Lett. 80 (1998) 1485.
- [23] S. Das Sarma, D.-W. Wang, Phys. Rev. Lett. 83 (1999) 816.
- [24] (a) P.A. Wolff, Phys. Rev. Lett. 16 (1966) 225. (b) P.A. Wolff, Phys. Rev. 171 (1968) 436. (c) F.A. Blum, Phys. Rev. B 1 (1970) 1125.
- [25] J.J. Sakurai, Advanced Quantum Mechanics, Addison-Wesley, Redwood, 1984.
- [26] A.L. Fetter, J.D. Walecka, Quantum Theory of Many-particle Systems, McGraw-Hill, San Francisco, 1971.
- [27] I.E. Dzyaloshinsky, A.I. Larkin, Zh. eksp. teor. Fiz. 65 (1973) 411 English translation: Soviet Phys. JETP 38, 202 (1974).
- [28] J. Hubbard, Proc. R. Soc. London Ser. A 243 (1957) 336.
- [29] H.J. Schulz, Phys. Rev. Lett. 71 (1993) 1864.
- [30] E.H. Lieb, F.Y. Wu, Phys. Rev. Lett. 20 (1968) 1445.
- [31] C.F. Coll, Phys. Rev. B 9 (1974) 2150.
- [32] C.N. Yang, Phys. Rev. Lett. 19 (1967) 1312.
- [33] (a) E.R. Gagliano, E. Dagotto, A. Moreo, Phys. Rev. B 34 (1986) 1677. (b) E.R. Gagliano, C.A. Balseiro, Phys. Rev. Lett. 59 (1987) 2999. (c) E.R. Gagliano, C.A. Balseiro, Phys. Rev. B 38 (1988) 11766. (d) E.R. Gagliano, C.A. Balseiro, Phys. Rev. Lett. 62 (1989) 1154.
- [34] (a) R. Preuss, A. Muramatsu, W. von der Linden, F.F. Assaad, W. Hanke, Phys. Rev. Lett. 73 (1994) 732. (b) M.G. Zacher, E. Arrigoni, W. Hanke, J.R. Schrieffer, Phys. Rev. B 57 (1998) 6370.
- [35] D.-W. Wang, A.J. Millis, S. Das Sarma, Phys. Rev. Lett. 85 (2000) 4570.
- [36] D.-W. Wang, S. Das Sarma, Phys. Rev. B 65 (2002) 125322.
- [37] However, we note that the SPE spectral weight near resonance depend on the actual value of λ in the present FL theory. IT actually diverges when λ is taken to be zero. Details is discussed in Ref. [38].
- [38] D.-W. Wang, A.J. Millis, S. Das Sarma, condmat/0405452.
- [39] We note that the Luttinger liquid theory is an effective low energy theory about the Fermi surface. Therefore in principle it is not appropriate for off resonance region, $\Omega > E_F$. But the resonance energy dependence may be still observable within the existing conditions of RRS experiments, say $0.1E_F < \Omega < E_F$.
- [40] (a) H.W. Yeom, K. Horikoshi, H.M. Zhang, K. Ono, R.I.G. Uhrberg, Phys. Rev. B 65 (2002) 241307. (b) T. Mizokawa, K. Nakada, C. Kim, Z.-X. Shen, T. Yoshida, A. Fujimori, S. Horii, Y. Yamada, H. Ikuta, U. Mizutani, Phys. Rev. B 65 (2002) 193101.
- [41] O.M. Auslaender, A. Yacoby, R. De Picciotto, K.W. Baldwin, L.N. Pfeiffer, K.W. West, Science 295 (2002) 825.
- [42] (a) Y. Tserkovnyak, B.I. Halperin, O.M. Auslaender, A. Yacoby, Phys. Rev. Lett. 89 (2002) 136805. (b) Y. Tserkovnyak, B.I. Halperin, O.M. Auslaender, A. Yacoby, Phys. Rev. B 68 (2003) 125312.
- [43] (a) H. Frahm, V. Korpein, Phys. Rev. B 42 (1990) 10553. (b) Phys. Rev. B 43 (1991) 5653.